Journal of Visualization, Vol. 11, No. 4 (2008)319-327

Regular Paper

Numerical Visualization of Vortex Flow Behavior in Square Jets in Cross-Flow

Maidi, M.* and Yao, Y.*

* Faculty of Engineering, Kingston University, 104 Friars Avenue, Roehampton Vale, London SW15 3DW, United Kingdom. E-mail: m.maidi@kingston.ac.uk, and y.yao@kingston.ac.uk

Received 5 November 2007
Revised 14 April 2008

Abstract : Direct numerical simulations have been performed in this study to visualize the flow behavior of single and multiple square jets issuing normally into a cross-flow. Three configurations are considered, a single jet located in the centre of the domain, twin jets in side-by-side (SBS) arrangement in the spanwise direction and triple jets in tandem arrangement with twin jets at the front and a third jet in downstream along the centre line. Simulation uses a jet to cross-flow velocity ratio of 2.5 and the Reynolds number 225, based on the free-stream quantities and the jet width. While the vortical structures predicted from single jet case were in good qualitatively agreement with the findings of other researchers, our results show that the process of merging between two counter-rotating vortex pairs (CRVP) in twin jets configurations is strongly dependent on the jet-to-jet edge distance. Further downstream in the far-field, results from the SBS twin jets show a most dominating larger CRVP accompanied with a smaller inner vortex pair. The observations are in good qualitative agreement with the experimental findings in the literature. The resulting flow structures of triple jets in tandem configuration have revealed, for the first time, more complicated flow interactions between individual jets and cross-flow, providing further insights of complex flow physics and its potential engineering applications.

Keywords : Direct numerical simulation, Jets in cross-flow, Vortex flow structure and interaction.

1. Introduction

The behavior of normal jet in cross-flow (JICF) has been extensively investigated due to its wider engineering and industrial applications involving mixing and pollutant dispersion from chimney stacks, film cooling of turbine blades, V/STOL aircraft and numerous manufacturing processes. An extensive review was given by Margason (1993), covering fifty years of JICF researches up to 1993.

By using smoke-wire visualization techniques, Fric and Roshko (1994) identified the complex vortex system associated with JICF and described their findings with four main vertical structures, namely the horseshoe vortex, the jet shear layer vortex, the wake vortex, and the counter rotating vortex pairs (CRVP). The horseshoe vortex forms upstream of the jet exit and wrapping around the exiting jet orifice. The jet shear layer consists of the vortex rollers in upstream side of the jet. The wake vortex forms downstream of the jet column, and persists and convectively transports further downstream. The CRVP which is originated as an effect of the bending of the jet itself constitutes the dominant structure in the JICF. These observations were later confirmed by other researchers (e.g., Lozano et al., 1994; Eiff et al., 1995; Smith and Mungal, 1998).

Although the single JICF has been studied for decades, the origin and dynamics of the complex flow structures are still not completely understood yet. The problem becomes even more complicated while considering the multiple jets, which are widely used in engineering applications. However the available results in public domain are very limited. In brief, Ziegler and Wooler (1971) proposed a physical model to study the flow of double jet system exhausting normally into cross-flow with side-by-side and tandem orientations. They assumed that the jet deflection was mainly due to the entrainment of mainstream fluid and the pressure forces acting on the boundary of the jet. Toy et al. (1993) also investigated the interactions of twin JICF side-by-side and inline. They reported that the mixing region in the far-field is similar in shape compared to single JICF but much larger in size.

While recent experiments have shed some new light upon the effects of large-scale structures in the JICF configuration, flow details remain unclear. On this aspect, numerical simulations could provide more complete information on the complex flow structures and their interactions. The modeling based CFD computations are generally unable to reproduce the complicated flow behavior accurately and the recent advancement in direct numerical simulations (DNS) methodology makes it feasible to obtain high quality database, which is often difficult or sometime even impossible to have at the laboratory conditions. Based on DNS data, the present paper will perform visualization study of the flow interactions in single and multiple JICF, with primary focus placing on the flow physics and the underlying mixing mechanisms.

2. Numerical Technique

In this study, the 3D compressible unsteady Navier-Stokes equations are numerically solved by using high-order finite-differences in space and multi-stage Runge-Kutta algorithm for time advancement. An entropy splitting concept is used to improve the stability of the numerical scheme (Sandham et al., 2002), and stable boundary treatment technique based on the summation by parts (SBP) approach of Carpenter et al. (1999) is adopted at the boundaries. More details of code description and numerical technique can be found in Sandham et al. (2002) and key numerical features are described in follows.

We are solving the non-dimensional Navier-Stokes equations in conservative forms as

$$\frac{\partial \rho}{\partial t} + \frac{\partial \rho u_j}{\partial x_j} = 0, \tag{1}$$

$$\frac{\partial \rho u_i}{\partial t} + \frac{\partial \rho u_i u_j}{\partial x_j} = -\frac{\partial p}{\partial x_i} + \frac{1}{\mathrm{Re}}\frac{\partial \tau_{ij}}{\partial x_j}, \tag{2}$$

$$\frac{\partial E}{\partial t} + \frac{\partial (E+p)u_j}{\partial x_j} = \frac{\partial u_i \tau_{ij}}{\partial x_j} + \frac{1}{(\gamma-1)\,\mathrm{Re}\ \mathrm{Pr}\ M^2}\frac{\partial}{\partial x_j}\left(\mu\frac{\partial T}{\partial x_j}\right), \tag{3}$$

where τ_{ij} represents shear stress tensor, Re the Reynolds number, γ the specific heats, Pr the Prandtl number, M the Mach number, and μ the dynamic viscosity. All other variables follow the standard notations as seen in Yao et al. (2006). The code was developed for compressible flow. In this application, we adopt low Mach number (~ 0.2) to reduce the compressibility effects.

The code has been parallelized using the MPI library and validated extensively for numerous configurations including laminar boundary layer and channel flows (Yao et al., 2000), turbulent boundary layer (Yao et al., 2000), turbulent channel flows (Sandham et al., 2002; Hu et al., 2003), transonic flow over a bump geometry with shock/boundary layer (Sandham et al., 2003) and most recently jet in cross-flow (Yao et al., 2006).

3. Problem Configuration

The problem configuration used in the simulations consists of square jets issuing perpendicularly into main cross-flow. For single jet case, the computational box combines a rectangular cross-flow domain with a dimension of 24D × 8D × 6D in longitudinal, wall-normal and transverse directions, respectively, and a jet domain of 1D × 1D × 1D, with D the jet width. The jet is located in [4D, 5D] from the cross-flow inlet plane in the streamwise direction and [2.5D, 3.5D] in the spanwise direction, respectively (see Fig. 1). The lateral spacing of 6D was primarily based on an existing numerical of this kind (Sau et al., 2004) and further confirmed by our numerical study on domain influence study.

The computational grid has 241 points in the streamwise (with 11 points in the jet domain), 81 points in the wall-normal and 61 points in the spanwise direction (with 11 points in the jet domain).

The twin JICF case consists of two jet domains (of same size as single jet case) arranged side-by-side in the spanwise direction with jet-to-jet edge distances of 2D and 1D. The spanwise of main computational domain is then increased to 91 and 81 points accordingly, while keeping the grid points in each jet domain and the distance of jets to the side-planes of the main domain (i.e., 2.5D) unchanged. Similar to that in single JICF case, the jets are located in [4D, 5D] from the cross-flow inlet plane in the streamwise direction. For triple jets in tandem case, an additional third jet was introduced along the centre line, with jet-to-jet edge distance of 2D to the trailing-edge of upstream twin jets of edge distance of 1D. The cross-flow velocity profile is initialized using a similarity solution of laminar boundary-layer at the Reynolds number of 225 and a Poiseuille-type profile is given at the inlet of jet orifice. The characteristics boundary conditions are used at both outlet plane and upper surface, and periodic conditions for the side-planes. Simulations are performed for jet to cross-flow velocity ratio R = 2.5 and the Reynolds number Re = 225, based on the free-stream quantities of the cross-flow and the jet width (D) and Mach number $M = 0.2$, based on the free-stream quantities.

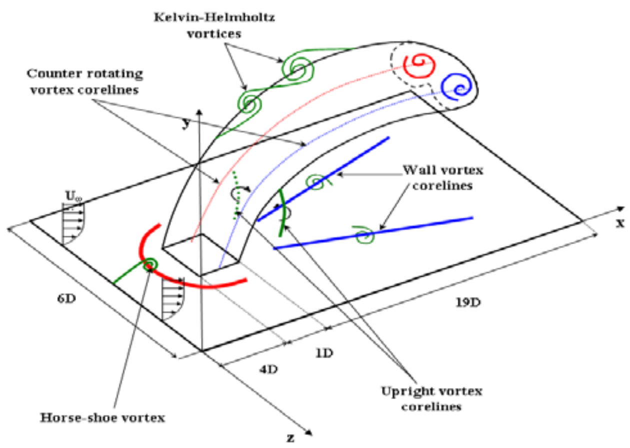

Fig. 1. A schematic view of large vortex structures in single JICF.

4. Results and Discussions

In the present study we present the results only at a particular instantaneous time of t = 18 since the main objective of the present work is to visualize the vortex flow structures. Discussions are focused on the underlying physical mechanism of single and multiple JICF.

We depict 3d iso-surface of spanwise vorticity (ω_z) and its 2d contours at mid-span plane in Fig. 2 for all four cases studied. In Fig. 2(a), the important flow feature which characterizes the interaction between the jet and the cross-flow is the formation of the streamwise counter-rotating vortex pair (CRVP) which dominates the flow field. These coherent structures constitute an obstacle and generate adverse pressure gradients which produce the horseshoe vortex that wraps around the edge of the jet hole (also see Fig. 3). This lateral deflection due to the jet vertical bending leads to the entrainment process of the cross-flow in the near wake region (at the trailing edge of the jet hole). Figure 2(b) reveals the presence of the shear layer vortex that emerges at the upstream side of the initial portion of the jet. The roll-up process of the shear layer upstream of the jet has been attributed to the Kelvin-Helmholtz (K-H) instabilities (Fric and Roshko, 1994; Kelso et al., 1996; Sau et al., 2004). One can see from Fig. 2(b) that the vortex rollers move downstream while merging with neighboring rollers, so that the scale of these K-H vortices increases with downstream distance as seen in free jet flow (Maidi and Lesieur, 2005). It is worth mentioning that Fig. 2(a) does not show any indication of the presence of the K-H rollers along the downstream side of the jet. This is in good agreement with DNS results of Sau et al. (2004), in which they found that the K-H vortices did not grow in the form of closed loop (ring-like) structures around the jet. Downstream of the jet exit, Figs.

3 and 5(a) also show the presence of so-called wake vortices from the downstream cross-flow shear layer. The vorticity in the wake region originates from the injection of wall boundary layer, where the boundary layer fluid wraps around the jet (Fric and Roshko, 1994). All these observations are in good agreement with previous experimental and numerical predictions (e.g., Fric and Roshko, 1994; Kelso et al., 1996; Lim et al., 2001; Sau et al., 2004; Ramesh et al., 2006).

We continued the visualization by focussing on the vortex structures of twin JICF and the discussion on its physical mechanisms of flow interactions, by extending our know knowledge from single to twin JICF configurations. Figures 2(c) and (e) show the resulting 3d iso-surfaces of spanwise vorticity and their corresponding streamlines in Figs. 5(b) and (c) for two cases of the jet-to-jet edge distances of 2D and 1D, respectively. Initially, the two jets produce two independent CRVPs similar to that observed in single JICF. Further downstream, two CRVPs attract each other and start to merge. As shown, the merging mechanism between two CRVPs depends strongly on the jet-to-jet edge distance. At relatively large edge distance of 2D, the merging process starts later at about x = 20D, while with small edge distance of 1D, the two CRVPs start to merge earlier at about x= 10D. This feature is also clearly seen in Figs. 2(d) and (f), showing the spanwise vorticity contours in a vertical median plane between two jets. Further downstream after merging, the flow is shown to be dominated by only a single CRVP (see Figs. 4(b) and (d)). It is worth noting that due to the strong intermittent interaction between two jets, the Kelvin-Helmholtz rollers in the upstream side of the jets are not clear in the case of small edge distance of 1D (see Fig. 2(e)). Figures 4(a) – (d) show contours of the streamwise vorticity in the y-z plane at two successive x-locations. Figure 4(a) indicates that the flow between two jets has been largely disturbed and the jet flow tends to bend towards each other as a result of the entrainment. Similar behaviour of vortex dynamics is found in the case of small edge distance of 1D (see Fig. 4(c)). Nevertheless the interactions between two jets exhibit more complicated patterns than single jet. Figures 4(a) and (c) also indicate that two CRVPs are quenched and led to one inner vortex pair in the near wall region. This small and less energetic inner vortex pair seems to not survive for long and is dissipated quickly before leaving the computational domain, as seen in Figs. 4(b) and (d), where only a single dominant CRVP exists. This finding agrees well with the laboratory measurements of Toy et al. (1993).

We finally moved on to the visualization of vortex structure in the case of triple JICF in tandem configuration. Compared to those twin JICF cases, the simulated 3d iso-surfaces in Fig. 2(g) and corresponding 3d streamlines in Fig. 5(d) show even more complicated flow interactions between three jets and cross-flow. Figure 6 provides further information in complementary to that by Figs. 2(g) and 5(d), showing that the lateral spreading of the rear third jet seems to be more significant than that in single jet case. This is mainly due to the strong interactions between two front jets and the rear jet. This phenomena can be clearly seen in Figs. 4(e) and (f) that show the contours of streamwise vorticity in the (y, z) plane at two downstream locations of x = 18D and x = 23D. Indeed, Fig. 4(e) revels that, the flow field is dominated by a large mushroom-shaped CRVP located in the middle of the domain. This central CRVP undergoes a merging process with two smaller side vortex pairs (originated from the upstream side-by-side twin jets) with same signs so that the scale and the lateral spreading of the large CRVP grow with the streamwise distance. Such merging and pairing between large CRVP and their neighbouring small vortex pairs with same signs have led to the helical distortion and tilting of the side jet flows as seen in Fig. 4(e). Finally, the flow field close to the domain exit is seen to be governed by a large CRVP in the middle of the domain with other smaller side vortex pairs persisting far downstream. Compared to single JICF, Fig. 2(h) has shown that the K-H rollers form earlier in the upstream shear layer of the rear third jet. Further downstream, these vortex pairs undergo several merging and pairing process, similar to that in the single JICF. The earlier appearance of the K-H rollers can be attributed to the perturbations caused by the twin jets in upstream.

5. Conclusions

The interactions between single and multiple jets with cross-flow are examined using direct numerical simulation (DNS) approach. A total of four cases are considered, i.e., single jet, twin jets in side-by-side arrangement with the jet-to-jet edge distance of 2D and 1D (with D the jet width) and triple jets in tandem arrangement with twin jets of the edge distance of 1D in the spanwise in upstream and a third jet of the edge distance of 2D in the streamwise in downstream.

For single JICF, the resulting vortex structures were in good agreement with both experiments and other numerical simulations in the literature. The computations successfully reproduced the important vortex patterns presented in this type of flow, including the counter-rotating vortex pair (CRVP), horseshoe vortex, shear layer vortex and wake vortex.

The flow features of twin JICF show that downstream of the jets, the merging between two CRVPs is strongly dependent on the jet-to-jet edge distance. At the edge distance of 1D, the merging process starts earlier than that in the case of edge distance of 2D. Further downstream, the flow is shown to be dominated by one single CRVP for both cases considered. Our simulations also identified the presence of an inner vortex pairs accompanying a primary CRVP. The inner vortex pair is small and less energetic, thus it does not survive for longer and is dissipated quickly downstream. Simulation results are in good qualitative agreement with the experimental findings in the literature.

The simulated flow structures associated with triple JICF in tandem show further complicated flow interactions between three jets and cross-flow. The downstream flow field is seen to be dominated by a large mushroom-shaped CRVP located in the middle of the domain with other smaller side vortex pairs in nearby. The observation obtained from the study would be valuable for both in-depth flow physics research and as well as in-width practical industrial applications.

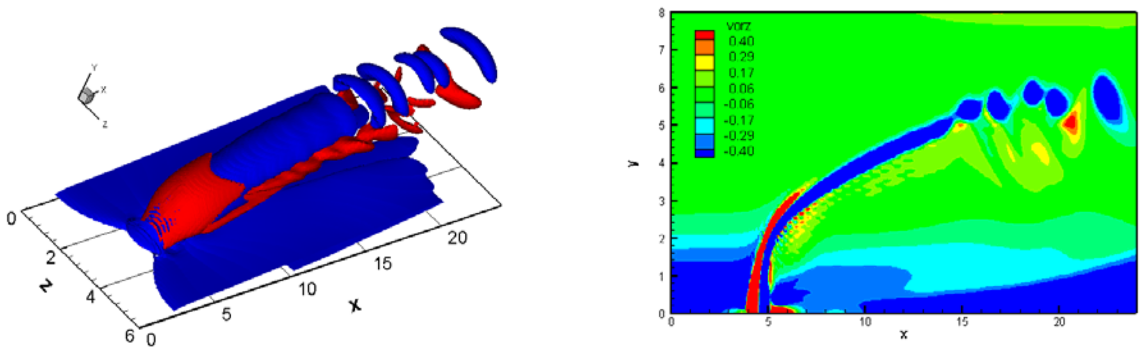

(a) (b)

Single JICF

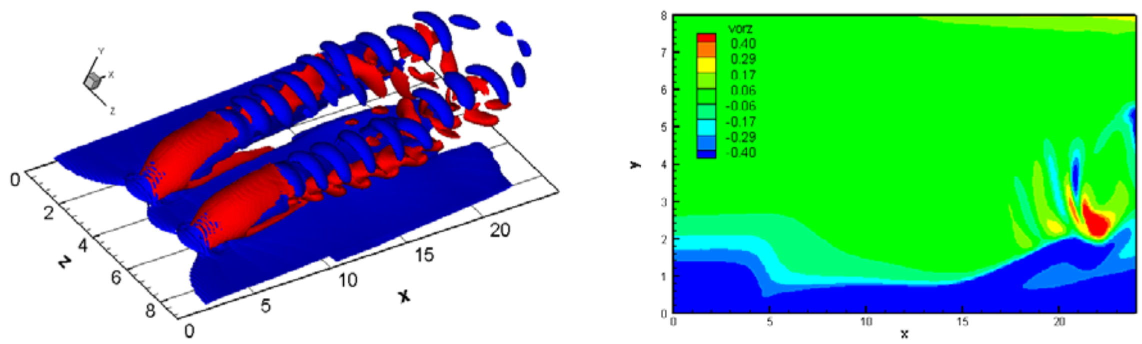

(c) (d)

Twin JICF with jet-to-jet edge distance of 2D

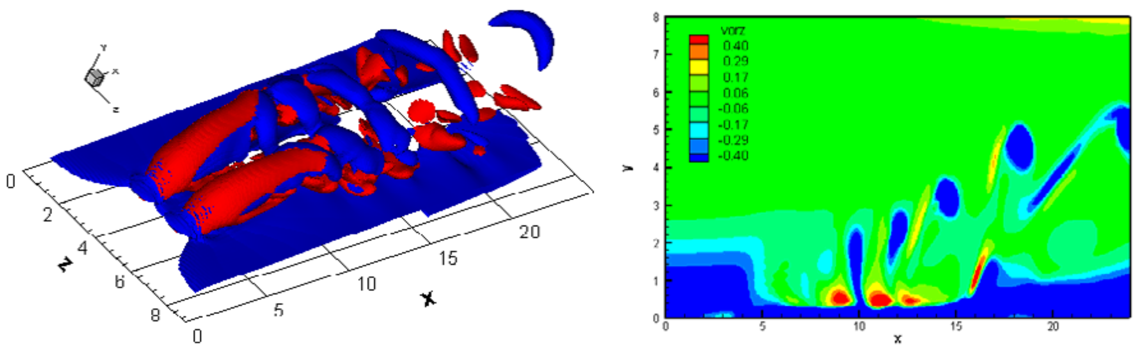

(e) (f)

Twin JICF with jet-to-jet edge distance of 1D

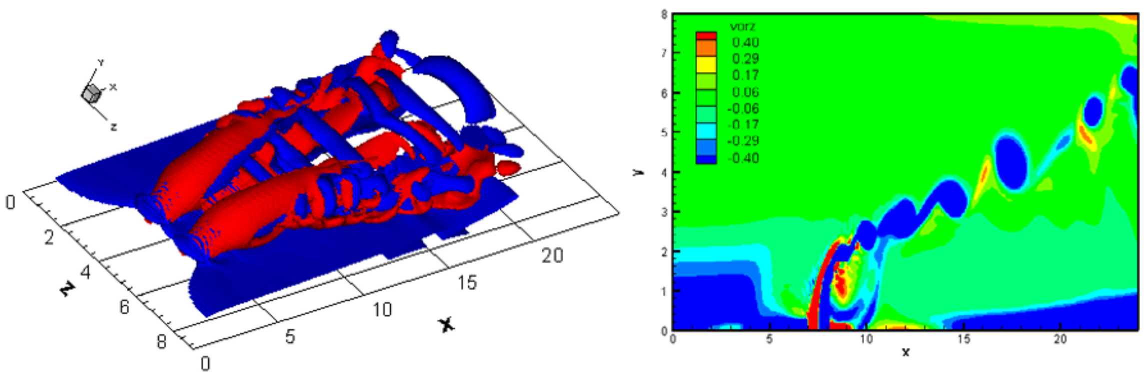

(g) (h)

Triple JICF in tandem arrangement

Fig. 2. Simulated 3d iso-surfaces of the spanwise vorticity (ω_z= ±0.5, red positive and blue negative) (left) and 2d contours of the spanwise vorticity at a median vertical plane (right).

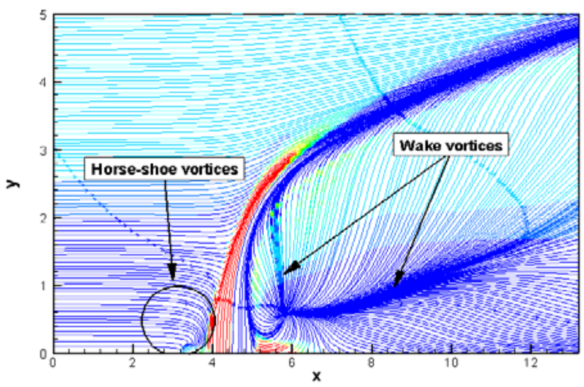

Fig. 3. Simulated streamlines coloured by the spanwise vorticity (ω_z = ±0.5, red positive and blue negative) at the median vertical plane from the single JICF.

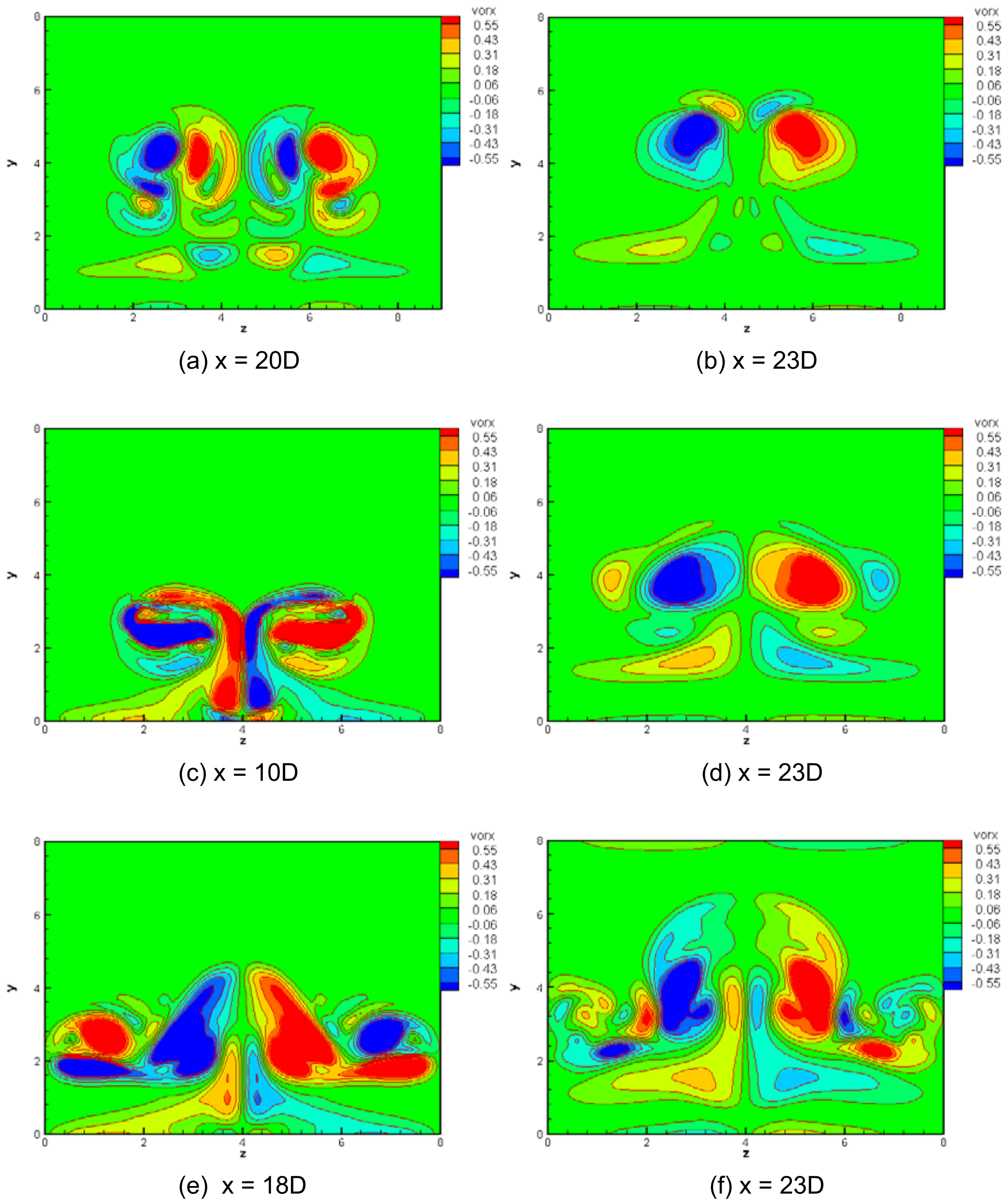

(a) x = 20D (b) x = 23D

(c) x = 10D (d) x = 23D

(e) x = 18D (f) x = 23D

Fig. 4. Contours of the streamwise vorticity at two successive streamwise x-locations. Twin jets with edge distance of 2D (top), twin jets with edge distance of 1D (middle) and triple jets in tandem (bottom).

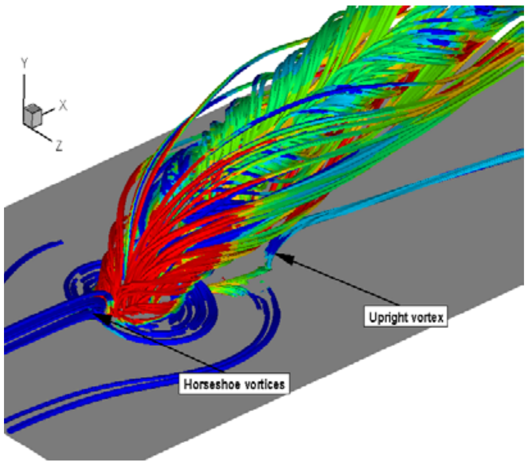

(a) Single JICF

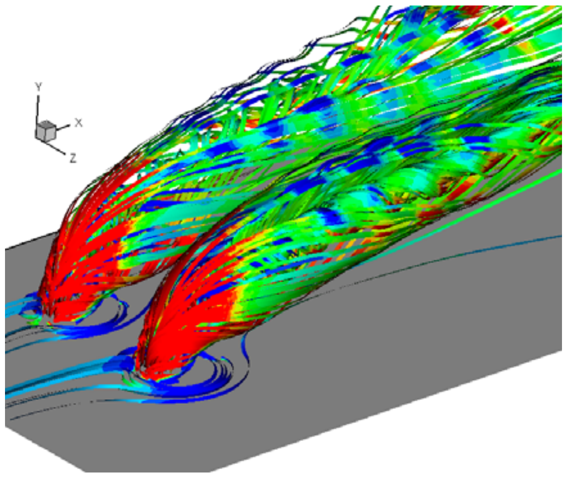

(b) Twin JICF with edge distance of 2D

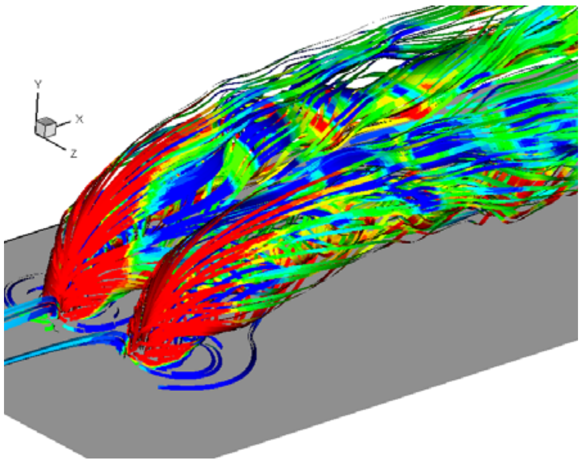

(c) Twin JICF with edge distance of 1D

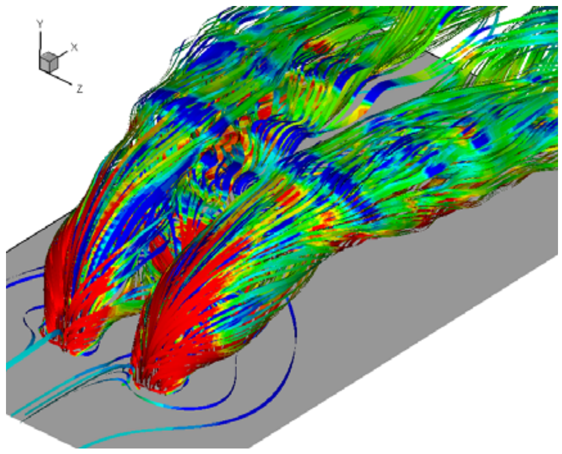

(d) Triple JICF in tandem

Fig. 5. The 3d streamlines coloured by the spanwise vorticity ($\omega_z = \pm 0.5$, red positive and blue negative).

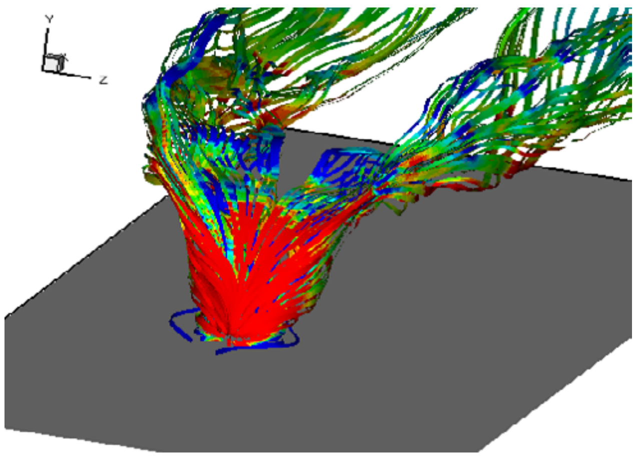

Fig. 6. The 3d streamlines of the third jet the case of triple JICF in tandem coloured by the spanwise vorticity ($\omega_z = \pm 0.5$, red positive and blue negative), in the absence of the front twin jets.

Acknowledgements

The authors would like to acknowledge the financial support from the UK Engineering and Physical Science Research Council (EPSRC) through research grant EP/C014979/1.

References

Carpenter, M. H., Nordstrom, J. and Gottlieb, D., A stable and conservative interface treatment of arbitrary spatial accuracy, J. of Comp. Phys., 148-2 (1999), 341-365.

Eiff, O. S., Kawall, J. G. and Keffer, J. F., Lock-in of vortices in the wake of an elevated round turbulent jet in a crossflow. Exps. Fluids, 19 (1995), 203-213.

Fric, T. F. and Roshko, A., Vortical structure in the wake of a transverse jet, J. Fluid Mech., 279 (1994), 1-47.

Hu, Z., Morfey, C. L. and Sandham, N.D., Sound radiation in turbulent channel flows, J. Fluid Mech., 475 (2003), 269-302.

Kelso, R. M., Lim, T. T. and Perry, A. E., An experimental study of round jets in cross-flow. J. Fluid Mech., 306 (1996), 111-144.

Lim, T. T., New, T. H. and Luo, S. C., On the Development of Large-scale Structures of a Jet Normal to a Cross Flow. Physics of Fluids, 13 (2001), 770-775.

Lozano, A., Smith, S. H., Mungal, M. G. and Hanson, R. K., Concentration measurements in a transverse jet by planar laser-induced fluorescence of acetone, AIAA J., 32 (1994), 218-221.

Maidi, M. and Lesieur, M., Large eddy simulations of spatially growing subsonic and supersonic turbulent round jets, Journal OF Turbulence, 6-38 (2005), 1-20.

Margason, R. J., Fifty year of jet in cross flow research, AGARD-CP-534, (1993), 1.1-1.41.

Ramesh, G., Venkatakrishnan, L. and Praghu, A., PIV studies of large scale structures in the near field of small aspect ratio elliptic jets, Journal of Visulization, 9-1 (2006), 23-30.

Sandham, N.D., Li, Q. and Yee, H. C., Entropy splitting for high-order numerical simulation of compressible turbulence, J. of Comp. Phys., 178 (2002), 307-322.

Sandham, N.D., Yao,Y. F. and Lawal,A. A., Large-eddy simulation of transonic turbulent flow over a bump, Int. J. of Heat and Fluid Flow, 24-4 (2003), 584-595.

Sau, A., Sheu, T. W., Hwang, R. and Yang, W. C., Three-dimensional simulation of square jets in cross- flow, Physical Review E, 69-6 (2004), Art. No. 066302.

Smith, S. H. and Mungal, M. G., Mixing structure and scaling of the jet in crossflow, J. Fluid Mech, 357 (1998), 83-122.

Toy, N., Savory, E., McCusker, S. and Disimile, P.J., The interaction region associated with twin jets and a normal crossflow, AGARD-CP-534, (1993), 7.1-7.10.

Ziegler, H. and Wooler, P. T., Multiple Jets Exhausting into a Crossflow, Journal of aircraft, 8-6 (1971), 414-420.

Yao, Y. F., Lawal, A. A., Sandham, N. D., Wolton, I. C., Ashworth, M. and Emerson, D. R., Massively parallel simulation of shock/boundary-layer Interactions, Proc. Inter. Conf. Applied Computational Fluid Dynamics (Beijing), (2000), 728–735.

Yao, Y., Petty, D., Barrington, P. E., Yao, J. and Mason, P. J., Direct Numerical Simulation of Jets in Cross-flow, International Journal of Computational Fluid Dynamics, 20-5 (2006), 279-285.

Author Profile

Mohamed Maidi: He received his M.Sc. (Eng) in Fluid Mechanics and Heat Transfers in 2001 from the Grenoble National Polytechnic Institute, France. He also received his Ph.D in Fluid Mechanics and Heat Transfers in 2004 from the Grenoble National Polytechnic Institute. He worked in the French Center for Scientific Research (Grenoble and Paris) as a Post-doctorate researcher between 2004 and 2006. He now works in the Aerospace Research Centre, Kingston University, UK as a Research Fellow since 2006. His research interests are computational aerodynamics, computational fluid mechanics, turbulence simulation and modeling and high performance computing.

Yufeng Yao: He received his M.Sc. (Eng) degree in Aeronautical Engineering from Nanjing University of Aeronautics and Astronautics, China in 1987 and Ph.D in Aerospace Engineering from Glasgow University in 1996. He then worked as Research Fellow at the Department of Engineering, Queen Mary and Westfield College, University of London 1996-99 and the School of Engineering Sciences, University of Southampton 1999-2002. Later he worked shortly with Siemens power generation section as Senior Aero-thermal Engineer, before joining Kingston University as Senior Lecturer in Aerospace Engineering He is currently Reader in CFD, with research interests in computational aerodynamics and fluid mechanics, turbulence simulation and modeling, two-phase flow and multi-scale modeling.